

# UC Davis

## UC Davis Previously Published Works

### Title

A new dual stainless steel cryogenic trap for efficient separation of krypton from argon and xenon

### Permalink

<https://escholarship.org/uc/item/3xw385xr>

### Journal

Journal of Analytical Atomic Spectrometry, 35(11)

### ISSN

0267-9477 1364-5544

### Authors

Péron, Sandrine  
Mukhopadhyay, Sujoy  
Huh, Michael

### Publication Date

2020-09-17

### DOI

10.1039/D0JA00052C

### Supplemental Material

<https://escholarship.org/uc/item/3xw385xr#supplemental>

### Data Availability

The data associated with this publication are within the manuscript.

Peer reviewed

# JAAS

Journal of Analytical Atomic Spectrometry

Accepted Manuscript

This article can be cited before page numbers have been issued, to do this please use: S. Péron, S. Mukhopadhyay and M. Huh, *J. Anal. At. Spectrom.*, 2020, DOI: 10.1039/D0JA00052C.



This is an Accepted Manuscript, which has been through the Royal Society of Chemistry peer review process and has been accepted for publication.

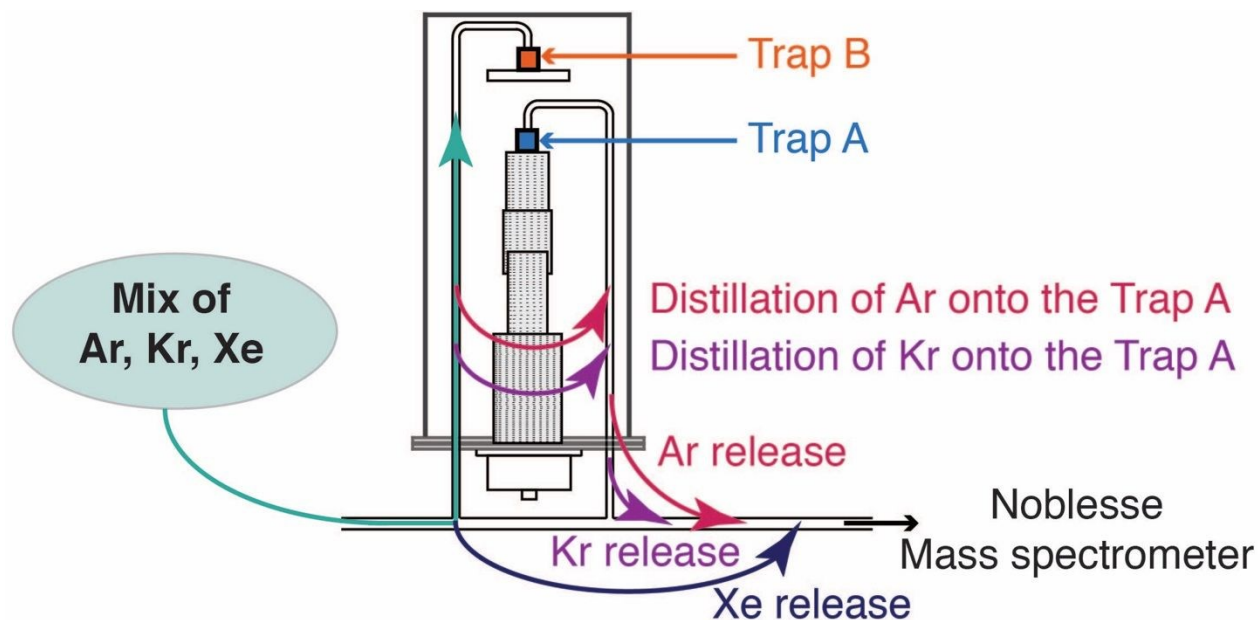
Accepted Manuscripts are published online shortly after acceptance, before technical editing, formatting and proof reading. Using this free service, authors can make their results available to the community, in citable form, before we publish the edited article. We will replace this Accepted Manuscript with the edited and formatted Advance Article as soon as it is available.

You can find more information about Accepted Manuscripts in the [Information for Authors](#).

Please note that technical editing may introduce minor changes to the text and/or graphics, which may alter content. The journal's standard [Terms & Conditions](#) and the [Ethical guidelines](#) still apply. In no event shall the Royal Society of Chemistry be held responsible for any errors or omissions in this Accepted Manuscript or any consequences arising from the use of any information it contains.

**Table of contents Entry**

We use a new cryogenic system and a new protocol to achieve efficient krypton separation from argon and xenon.



1  
2  
3  
4  
5  
6  
7  
8  
9  
10  
11  
12  
13  
14  
15  
16  
17  
18  
19  
20  
21  
22  
23  
24  
25  
26  
27  
28  
29  
30  
31  
32  
33  
34  
35  
36  
37  
38  
39  
40  
41  
42  
43  
44  
45  
46  
47  
48  
49  
50  
51  
52  
53  
54  
55  
56  
57  
58  
59  
60

1  
2  
3  
4  
5  
6  
7  
8  
9  
10  
11  
12  
13  
14  
15  
16  
17  
18  
19  
20  
21  
22  
23  
24  
25  
26  
27  
28  
29  
30  
31  
32  
33  
34  
35  
36  
37  
38  
39  
40  
41  
42  
43  
44  
45  
46  
47  
48  
49  
50  
51  
52  
53  
54  
55  
56  
57  
58  
59  
60

1 **Title:** A new dual stainless steel cryogenic trap for efficient separation of krypton from argon and xenon

View Article Online  
DOI: 10.1039/C9JA00052C

2  
3  
4 **Authors:** Sandrine Péron<sup>1\*</sup>, Sujoy Mukhopadhyay<sup>1</sup> and Michael Huh<sup>1</sup>

5  
6 **Affiliations:** <sup>1</sup>Department of Earth and Planetary Sciences, University of California - Davis,  
7 Davis, California 95616, USA

8  
9 \* corresponding author: [scperon@ucdavis.edu](mailto:scperon@ucdavis.edu)

### 10 **Abstract:**

11 The elemental and isotopic abundances of krypton and xenon provide critical insights into  
12 processes ranging from stellar nucleosynthesis to volatile accretion and paleotemperatures on  
13 Earth. Accurate and precise determination of the krypton and xenon elemental abundance and  
14 isotopic ratios requires sample purification and noble gas separation to avoid interferences in  
15 the mass spectrometer. However, effective separation of krypton (Kr) from argon (Ar) and  
16 xenon (Xe) has remained challenging. Here, we present a new cryogenic instrument associated  
17 with a new protocol to achieve an efficient and effective separation of Kr from Ar and Xe.  
18 Using two electropolished stainless steel cryogenic traps on a single cold head, distillation of  
19 the noble gases from one trap onto the other and temperature cycling of the traps to reduce the  
20 effect of cryotrapping allows  $\geq 98\%$  of the Kr in a sample to be recovered with  $< 0.5\%$  of the  
21 Ar and  $< 1\%$  of the Xe abundances of the sample. Likewise, more than 99 % of the Xe fraction  
22 can be recovered with  $< 1\%$  Kr. No variations in the isotopic ratios of the separated Kr and Xe  
23 fractions are observed as a function of the signal size for air standards. Moreover, we find that  
24 krypton isotopes can be fractionated during Ar-Kr separation. We suggest that more accurate  
25 krypton isotopic compositions can be obtained by maximizing the recovered krypton fraction  
26 instead of minimizing the argon fraction within krypton.

### 27 **Introduction**

28  
29  
30 Noble gases (helium, neon, argon, krypton and xenon) are invaluable tracers due to their  
31 inertness and as a consequence are used for a wide range of applications in Earth and planetary  
32 sciences including geochronology, hydrology, paleoclimatology, cosmochemistry and mantle  
33 geochemistry (1–3). Among the 22 noble gas isotopes, some are primordial in the Earth's  
34 mantle (e.g., <sup>3</sup>He, <sup>20</sup>Ne, <sup>38</sup>Ar, <sup>124</sup>Xe), some are produced by cosmic rays on planetary surfaces  
35 (such as <sup>3</sup>He, <sup>21</sup>Ne), some are radiogenic (such as <sup>40</sup>Ar produced on Earth from the decay of  
36 <sup>40</sup>K, or <sup>129</sup>Xe produced from the decay of now extinct <sup>129</sup>I) and others are fissionogenic (as  
37 <sup>131-132-134-136</sup>Xe produced by fission of extinct <sup>244</sup>Pu and extant <sup>238</sup>U). Since noble gases do not react  
38 with their environments in near-surface conditions, elemental and isotopic ratios of primordial  
39 isotopes are key tracers of volatile sources on terrestrial planets, whereas cosmogenic,  
40 radiogenic and fissionogenic isotopes have proved to be useful dating tools for early Solar System  
41 processes, terrestrial climatic and tectonic processes, and planetary degassing events (1–5).  
42 Noble gases hence offer a powerful way to understand formation of planets and their subsequent  
43 evolution.

44  
45  
46 Noble gas analyses are often challenging due to very low abundances, isobaric interferences  
47 (e.g., <sup>40</sup>Ar<sub>2</sub><sup>+</sup> with <sup>80</sup>Kr<sup>+</sup>) and varying mass discrimination effects due to changes in partial  
48 pressures in the mass spectrometer. As an example, the concentrations of <sup>36</sup>Ar, <sup>84</sup>Kr and <sup>130</sup>Xe  
49 in the atmosphere are of  $9.58 \times 10^{-13}$  mol/g,  $1.98 \times 10^{-14}$  mol/g and  $1.08 \times 10^{-16}$  mol/g, respectively,  
50

1  
2  
3 51 whereas in the bulk Earth's mantle there are estimated to be of  $7.8 \times 10^{-14}$  mol/g,  $1.9 \times 10^{-15}$  mol/g and  $2.6 \times 10^{-17}$  mol/g, respectively (6). With the exception of resonance ionization mass spectrometry (7,8), isotopic analyses of noble gases mostly involve mass spectrometers equipped with electron bombardment sources and magnetic sector filters (9). This type of ionization source shows strong dependence on partial pressure, as variations in partial pressure can significantly affect the mass spectrometer sensitivity and mass discrimination (9). Therefore, sample purification followed by separation of the five noble gases (He, Ne, Ar, Kr, Xe) from one another before sequentially introducing them into the mass spectrometer are generally considered best practices for reliable noble gas analyses.

4  
5  
6  
7  
8  
9  
10  
11  
12  
13  
14  
15  
16  
17  
18  
19  
20  
21  
22  
23  
24  
25  
26  
27  
28  
29  
30  
31  
32  
33  
34  
35  
36  
37  
38  
39  
40  
41  
42  
43  
44  
45  
46  
47  
48  
49  
50  
51  
52  
53  
54  
55  
56  
57  
58  
59  
60  
61  
62  
63  
64  
65  
66  
67  
68  
69  
70  
71  
72  
73  
74  
75  
76  
77  
78  
79  
80  
81  
82  
83  
84  
85  
86  
87  
88  
89  
90  
91  
92  
93  
94  
95  
96  
97  
98  
99  
100  
Samples are commonly purified through a series of hot and cold getters to remove reactive species (e.g.,  $\text{CO}_2$ ,  $\text{H}_2\text{O}$ ,  $\text{N}_2$ , etc) (e.g., 9). After purification, noble gases are cryogenically separated by being adsorbed at very low temperature (as low as 15 K) onto a substrate, usually activated charcoal, and sequentially desorbed in order of mass by increasing the temperature (9–11). The disadvantages of activated charcoal are the significant overlaps between the release curves of argon, krypton and xenon (e.g., 12), rendering the complete separation of Ar-Kr-Xe very difficult, if not impossible. The separation of the heavy noble gases thus often involves two separate traps to partition the gases (13). First, all the heavy noble gases are trapped on one trap. The temperature of this first trap is then set to partially desorb Ar, in order to progressively transfer Ar by distillation onto the second trap, which is kept at liquid nitrogen temperature (i.e., 77 K, temperature to which 100 % of Ar, Kr and Xe are adsorbed on charcoal) or lower. The same procedure is then repeated to separate Kr from Xe (13). Even with this protocol, significant amounts of argon can still be present in the krypton and xenon fractions due to the overlap in the release curves (e.g., 12), making krypton and xenon analyses difficult, krypton and xenon being typically two to five orders of magnitude less abundant than argon. Other variants of this procedure involve for example using two charcoal traps, one operating at 148 K for trapping Kr and Xe and the other operating at 77 K for trapping Ar, the noble gases are separated into three fractions – He/Ne, Ar, Kr/Xe (14,15). Alternatively, Kr and Xe are trapped onto a quartz finger at liquid nitrogen temperature while Ar mostly stays in the gas phase (16,17) although it is not completely clear what fraction of the Ar gets trapped with Kr and Xe. In both these cases, Kr and Xe have to be simultaneously admitted into the mass spectrometer and analyzed together, which can generate lower measurement precisions due to quick consumption by ionization in the mass spectrometer (typically half of the Kr, Xe signals can decrease in 30 minutes given the source parameters).

Some of the limitations of the charcoal trap can be overcome using a polished stainless steel trap (12). This type of trap shows steeper release curves and lower release temperatures compared to charcoal traps, allowing for significantly better separation of the heavy noble gases (12,18,19). However, even with a stainless steel trap, there is still overlap between the Ar, Kr and Xe release curves and the use of a single trap does not allow proper separation of the heavy noble gases (12,18,19). Hence, a new cryogenic system was designed with two stainless steel traps on a single cryogenic head and a technique was developed to effectively separate Ar from Kr from Xe.

### **Apparatus design and experimental procedure**

A new cryogenic system was fabricated by Janis Research Company for the UC Davis Noble Gas Laboratory (Figures 1 and S1 in Supplementary). The system uses a 4 K cold head with 0.5 W cooling power available on the second stage at 4.2 K (Sumitomo Model RDK-205J). There are two electropolished stainless steel traps associated with the cold head, one attached

1  
2  
3 101 to the second stage of the cold head with a high temperature stage and the second trap on the  
4 102 radiation shield; the radiation shield provides the thermal link between the trap and the first  
5 103 stage of the cold head (Figure 1). The two traps have independent silicon diode temperature  
6 104 sensors and heaters. For safety, the heaters are interfaced with a temperature sensor on the first  
7 105 stage of the cold head, so that heater power is automatically cut off when the cold head first  
8 106 stage reaches 290 K. The trap on the second stage of the cold head can be cooled down to < 5  
9 107 K (lowest achieved temperature was 4.7 K), hereafter named Trap A, and can reach a  
10 108 temperature of 500 K for bakeout. The trap on the radiation shield achieves temperatures of <  
11 109 50 K (lowest achieved temperature was 31 K), hereafter named Trap B, and can reach  
12 110 temperatures of 500 K for bakeout. The temperature on the two traps can be controlled  
13 111 independently, with no observable temperature feedback between them. For example, Trap B  
14 112 can be held at 200 K and the Trap A temperature can be easily controlled between 200 K and 5  
15 113 K. The two traps are controlled by a Lakeshore Model 335 temperature controller that interfaces  
16 114 with an Omega iSeries temperature controller used for monitoring the temperature of the first  
17 115 stage of the cold head. The Lakeshore controller interfaces with control computer of the vacuum  
18 116 line through a General Purpose Interface Bus.

19 117  
20 118 On Trap A, neon is completely adsorbed at 10 K, allowing a significant temperature buffer to  
21 119 counter the long-term degradation of the cold head. The Trap A can be cooled down from 200  
22 120 K to 8 K in less than 30 minutes. Likewise, the Trap B can be cooled down from 200 K to 70  
23 121 K in less than 30 minutes. Additionally, the Trap A can be cooled from 110 K to 6 K in 10  
24 122 minutes. The rapid cooling times allow for significant shortening of sample processing times.  
25 123 We also note that no pre-cooling time is needed, whereas charcoal cryogenic system often  
26 124 requires 30 minutes to 1 hour before starting the analysis to cool the system from 375 K (Xe  
27 125 release temperature) to about 15 K.

28 126  
29 127 We first obtained the release curves for Ne, Ar, Kr and Xe from a single trap (Figure 2). These  
30 128 release curves were similar to that previously determined for a stainless steel trap (12,19). For  
31 129 example, neon was completely adsorbed at 10 K, argon at 55 K, krypton at 70 K and xenon at  
32 130 90 K (Figure 2). The temperatures at which more than 99 % of Ne, Ar, Kr and Xe are released  
33 131 were 22 K, 83 K, 100 K and 135 K (Figure 2, Protocol 1, see below), respectively, in very good  
34 132 agreement with previous observations (12). Helium started to be adsorbed at 7.5 K.

35 133  
36 134 Based on the release curves (Figure 2), three different protocols, described below and in Figure  
37 135 3, are tested to efficiently separate Ar, Kr and Xe from each other. In the first protocol, an  
38 136 aliquot of an air standard is purified using a series of hot and cold MP10 SAES getters. After  
39 137 the purification, the noble gases are exposed to the Trap B set to 70 K to adsorb Kr and Xe. At  
40 138 70 K, a small fraction of Ar is also adsorbed (Figure 2). Then, the Trap A, set to 25 K, is opened  
41 139 to adsorb Ar for 10 minutes. During this process, as the Ar partial pressure decreases in the line  
42 140 due to Ar adsorption onto the 5K trap, Ar adsorbed on the 50K trap is progressively released  
43 141 and adsorbed on the Trap A. Both traps are closed and the line is pumped for 5 minutes and  
44 142 then opened again for 10 minutes to finish the transfer of Ar onto the Trap A, so that the total  
45 143 transfer duration of 20 minutes remains the same as for the second protocol (described below).  
46 144 Argon is then progressively released from the Trap A in steps of 2-5 K, inlet into the Noblesse  
47 145 (Nu Instruments) mass spectrometer and measured along with the Kr signal. Between each  
48 146 temperature step, the vacuum line and the mass spectrometer are pumped. After all the Ar is  
49 147 inlet into the mass spectrometer, Kr is distilled from the Trap B to the Trap A by setting the  
50 148 Trap B to 90 K and the Trap A to 70 K. Kr, and then Xe, can be desorbed from the Trap A and  
51 149 the Trap B, respectively, in temperature steps of 2-5 K. The release curves are determined by  
52 150 measuring Kr and Xe by mass spectrometry. While measuring the Kr abundance, Ar and Xe

151 abundances are also measured, and while measuring the Xe abundances, the Kr abundances are  
152 measured as well. View Article Online  
DOI: 10.1039/D0JA00052C

153  
154 In the second protocol, after Ar is frozen onto the Trap A, both traps are closed and the  
155 temperature of the Trap B is increased from 70 K to 120 K, held at 120 K for 5 minutes and  
156 then set back to 70 K. This temperature cycling is done to limit the effect of cryotrapping, which  
157 is the mechanism of one noble gas being trapped by another one (12,18). The temperature  
158 cycling allows the heavier noble gases to be layered beneath the lighter noble gases, making  
159 the separation of Ar, Kr, Xe more efficient (18). After this temperature cycle, both traps are  
160 opened so that the Ar that is no longer cryotrapped by Kr and Xe in the Trap B can be adsorbed  
161 onto the Trap A. After argon has been adsorbed onto the Trap A, the temperature of the Trap A  
162 is increased in steps of 2-5 K as per the first protocol, and the Ar abundance, as well as Kr  
163 abundance in the Ar fraction, are measured by mass spectrometry.

164  
165 Krypton is separated from xenon following the same principle. The Trap B is set to 90 K and  
166 the Trap A to 70 K. Both traps are opened to distill Kr from the Trap B onto the Trap A and  
167 then both traps are closed. The temperature of the Trap B is increased to 150 K, held at 150 K  
168 for 5 minutes and cycled back to 90 K to freeze Xe. Both traps are opened again to adsorb Kr  
169 initially cryotrapped by Xe onto the Trap A. Kr, and then Xe, can be desorbed from the Trap A  
170 and the Trap B, respectively, in temperature steps of 2-5 K in order to determine the release  
171 curves as well as Ar and Xe abundances with Kr and Kr abundance in the Xe fraction, as for  
172 the first protocol.

173  
174 In the third protocol, two temperature cyclings of the Trap B are performed to separate krypton  
175 from xenon (i.e., cycling the Trap B each time to 150 K and cycling it back to 90 K before  
176 opening the two traps for Kr distillation onto the Trap A).

177  
178 For the three protocols (Figure 3), the quantities of gas being processed in the line were of  
179  $3.8 \times 10^{-8} \text{ cm}^3$  of  $^{40}\text{Ar}$ ,  $2.38 \times 10^{-11} \text{ cm}^3$  of  $^{84}\text{Kr}$  and  $1.30 \times 10^{-13} \text{ cm}^3$  of  $^{130}\text{Xe}$ , that is comparable to  
180 the quantities of gas analyzed from basaltic glass samples for instance (20,21). The blank of the  
181 vacuum line is  $5.1 \times 10^{-10} \text{ cm}^3$  of  $^{40}\text{Ar}$ ,  $6.9 \times 10^{-15} \text{ cm}^3$  of  $^{84}\text{Kr}$  and  $4.4 \times 10^{-16} \text{ cm}^3$  of  $^{130}\text{Xe}$ , which  
182 is very low in comparison and can therefore be neglected in these experiments.

183  
184 We note that the release curves for the above experiments were determined by desorption of  
185 the gases at several temperature steps and inlet into the mass spectrometer, which corresponds  
186 to an effective distillation of the gas into the mass spectrometer. When a single temperature is  
187 chosen for desorbing a noble gas of interest, such as Kr or Xe, as is the case for processing most  
188 natural samples through the vacuum lines, the efficiency of separation would be expected to  
189 decrease. Hence, in another set of experiments, the effectiveness of the second protocol in  
190 separating Ar from Kr from Xe for natural samples is tested by desorption of the gases at single  
191 temperatures based on the release curves, using an air standard aliquot with  $1.7 \times 10^{-8} \text{ cm}^3$  of  
192  $^{40}\text{Ar}$ ,  $1.2 \times 10^{-12} \text{ cm}^3$  of  $^{84}\text{Kr}$  and  $6.6 \times 10^{-15} \text{ cm}^3$  of  $^{130}\text{Xe}$ . Following the temperature cycling and  
193 distillation process, argon was desorbed from the Trap A at 120 K, Kr from the Trap A at 140  
194 K and Xe from the Trap B at 160 K (Figure 2). Different distillation temperatures were tested,  
195 such as 67 K and 70 K to separate argon from krypton and 92 K and 95 K instead of 90 K to  
196 separate krypton from xenon. In the Ar fraction, the Kr abundance is monitored, in the Kr  
197 fraction, the Ar, Kr and Xe abundances are measured, while in the Xe fraction Kr and Xe  
198 abundances are measured.

199

1  
2  
3 200 In a final set of experiments, we investigated the influence of the argon partial pressure (as measured by the abundance of  $^{40}\text{Ar}$  in the mass spectrometer) on krypton isotopic ratios, using  
4 201 air standard aliquots with  $1.1 \times 10^{-7} \text{ cm}^3$  of  $^{40}\text{Ar}$ ,  $7.5 \times 10^{-12} \text{ cm}^3$  of  $^{84}\text{Kr}$  and  $4.1 \times 10^{-14} \text{ cm}^3$  of  $^{130}\text{Xe}$ .  
5 202 Krypton isotopic ratios were measured using distillation (second protocol described above and  
6 203 Figure 3) and different Ar-Kr distillation temperatures (from 67 K to 75 K) as well as using a  
7 204 single trap (Trap A) and no distillation. For the experiments with the single Trap A with no  
8 205 temperature cycling, the Ar-Kr separation temperature was varied from 68 K to 75 K. This  
9 206 allowed us to vary the argon partial pressure during krypton measurements by a factor of 22.  
10 207 We also carried out experiments with the same distillation temperature but with two distillations  
11 208 and one temperature cycle (Protocol 2 in Figure 3) as well as with three distillations and two  
12 209 temperature cycles for the separation of Ar from Kr in order to change the Ar partial pressure  
13 210 but not the Kr signal, and thus to further study the influence of the argon partial pressure.  
14 211  
15 212

16 213 The time to run a sample analysis is globally comparable between the use of a charcoal trap or  
17 214 a stainless steel trap. However, in detail, the time will be less for the dual trap if doing a single  
18 215 distillation without temperature cycle for Ar-Kr and Kr-Xe ( $\sim 3$  hours to run a sample),  
19 216 comparable if doing two distillations and one temperature cycle for Ar-Kr and Kr-Xe ( $\sim 4$  hours  
20 217 to run a sample), and more if three distillations and two temperature cycles are used ( $\sim 5$  hours  
21 218 to run a sample).  
22 219

23 220 For all measurements, Ar abundances were determined through measurement of  $^{40}\text{Ar}$ , Kr  
24 221 abundances through  $^{84}\text{Kr}$  and Xe abundances through  $^{129}\text{Xe}$  using the Nu Noblesse HR mass  
25 222 spectrometer equipped with five faraday cups and five electron multipliers. The mass  
26 223 spectrometer source is operated at 9KV and uses a yttrium coated tungsten filament for ionizing  
27 224 the noble gases. The mass spectrometer is fitted with two NP10 getters, two ion pumps and has  
28 225 an inline UHV all-metal valve that can be used to isolate the mass spectrometer source from  
29 226 the flight tube and detectors.  
30 227

31 228 Abundance of  $^{40}\text{Ar}$  was measured with one of the Faraday detectors while  $^{84}\text{Kr}$  and  $^{129}\text{Xe}$  were  
32 229 measured with an ion counter in pulse counting mode. The krypton isotopic ratios were  
33 230 measured during twelve cycles in three steps on the five electron multipliers. The first step was  
34 231 for determining the baselines of the collectors, the second step consisted of measuring  $^{78}\text{Kr}$ ,  
35 232  $^{80}\text{Kr}$ ,  $^{82}\text{Kr}$ ,  $^{84}\text{Kr}$  and  $^{86}\text{Kr}$  and the third step was for measuring  $^{83}\text{Kr}$ . The sensitivities of the  
36 233 Noblesse mass spectrometer at  $250 \mu\text{A}$  trap current and a filament voltage of  $-75 \text{ V}$  are typically  
37 234  $1.1 \times 10^{-7} \text{ cm}^3/\text{V}$  for  $^{40}\text{Ar}$ ,  $4.7 \times 10^{-16} \text{ cc/cps}$  for  $^{84}\text{Kr}$  and  $4.8 \times 10^{-16} \text{ cc/cps}$  for  $^{130}\text{Xe}$ .  
38 235  
39 236

## 40 236 **Results and discussion**

41 237  
42 238 The results of the three protocols used to separate krypton from argon and xenon in air standards  
43 239 are shown in figure 2 and in table 1. In figure 2, the release curves of Ar and Kr are very similar  
44 240 between the different protocols, as both noble gases are released from Trap A that did not have  
45 241 temperature cycle. For Xe, which is released from Trap B, the release curve obtained with no  
46 242 temperature cycle is shifted to the left compared to the release curve with temperature cycling.  
47 243 Xe appears more easily desorbed from the stainless steel trap when no temperature cycling is  
48 244 applied. Hence, this shift in Xe release highlights the need of carefully choosing a release  
49 245 temperature depending on the protocol applied.  
50 246

51 247 Table 1 lists the proportions of each gas remaining with the other gases with the different  
52 248 protocols. It is important to point out first that using only one stainless steel trap does not allow  
53 249 effective separation of Ar, Kr, Xe due to overlaps in the release curves (Table 1, row 1).  
54  
55  
56  
57  
58  
59  
60



250  
251 Using two traps improves the heavy noble gas separation and adding one temperature cycling  
252 procedure produces a further improvement in the separation (Table 1, rows 2-3). For example,  
253 the recovered Kr fraction (i.e., the percentage of Kr in the fraction primarily analysed for Kr)  
254 increases from 81.0 % to 96.2 % of the sample Kr abundance while the Ar in Kr decreases from  
255 2.7 % to 0.2 % of the sample Ar abundance. The Xe in Kr also decreases from 1.7 % to 1.4 %  
256 of the sample Xe abundance. Figure 4 shows the corresponding step-release of Ar, Kr and Xe  
257 with the respective abundances of other gases obtained for the three protocols (Table 1, rows  
258 2, 3, 4). This figure illustrates the significant improvement in the separation of Ar, Kr and Xe  
259 with the protocol with temperature cycling (i.e., the low proportions of other gases when  
260 releasing Ar, Kr or Xe).

261  
262 For the experiments where the Ar, Kr and Xe were desorbed at a single temperature, the  
263 effectiveness of the separation compared to observations from the release curves decreased  
264 slightly, but is nonetheless high (Table 1, row 3 vs. 5; step-release vs. single release for T1).  
265 The separation of krypton from argon and xenon can be even further improved. For example,  
266 doing two temperature cycles for Kr-Xe separation allows us to decrease the proportions of Kr  
267 in Xe and of Xe in Kr to less than 1 % (Table 1, row 4). Depending on the scientific objective,  
268 this second cycle can be important even if it is time-consuming; a full temperature cycle takes  
269 about 30 minutes to complete. Changing the release or freeze-down temperatures slightly is  
270 also interesting as it can increase the recovered proportion of Ar, Kr or Xe. For example,  
271 changing the distillation temperature of Ar from Kr from 70 K to 67 K increases the argon  
272 fraction into Kr to 0.5 % but lowers the krypton fraction into Ar to less than 1 % (Table 1, rows  
273 5-6). Setting the distillation temperature of Kr from Xe to 92 K or 95 K instead of 90 K allows  
274 the krypton fraction into Xe to be less than 1 % but increases the xenon fraction into Kr (Table  
275 1, rows 5-6). Therefore,  $\geq 99$  % of Ar,  $\geq 98$  % of Kr, and  $\geq 99$  % of Xe can be recovered from  
276 a sample with  $\leq 1$  % contribution from the other noble gases.

277  
278 We used the single temperature cycling protocol (Protocol 2, Figure 3) with a Ar-Kr distillation  
279 temperature of 67 K and a Kr-Xe distillation temperature of 92 K to verify that no mass  
280 fractionation effects as a function of signal size were introduced by the distillation process. The  
281 results obtained for krypton and xenon for air standards with such a protocol are shown in  
282 figures 5 and 6. The analyses are well reproducible and variations in mass discrimination are  
283 not observed over of range of Kr and Xe partial pressures. The measurement precision ranged  
284 from 0.16 % to 0.54 % for the  $^{78}\text{Kr}/^{84}\text{Kr}$  ratio and from 0.29 % to 1.19 % for the  $^{128}\text{Xe}/^{130}\text{Xe}$   
285 ratio.

286  
287 Figure 7 shows the evolution of the krypton isotopic ratios depending on the krypton trapping  
288 temperature and the argon partial pressure during measurements of air standard aliquots of the  
289 same size. For these experiments, the isotopic ratios are plotted normalized to the measured  
290 values of the air standard using both traps with a Kr trapping temperature of 68 K. The measured  
291 krypton isotopic ratios within uncertainties are consistent for a given krypton trapping  
292 temperature between the experiments using one and two traps. For instance, for a krypton  
293 trapping temperature of 68 K, the normalized  $^{86}\text{Kr}/^{84}\text{Kr}$  ratio is  $1.0013 \pm 0.0015$  ( $1\sigma$ ) using one  
294 trap and of  $1.0000 \pm 0.0016$  ( $1\sigma$ ) using two traps and a temperature cycling. The argon partial  
295 pressure for these two experiments varied by more than a factor of ten in the mass spectrometer  
296 ( $^{40}\text{Ar}$  of 78.8 mV and of 7.50 mV, respectively, Figure 7). Figure 7 shows that about a factor  
297 10 difference in the Ar partial pressure does not influence the measurement of Kr isotopes. This  
298 observation is confirmed for experiments with a varying number of distillations but with the  
299 same trapping temperature (Figure 8), where the measured Kr isotopic ratios are similar

300 whereas the Ar partial pressure changes by a factor of 1.8. Therefore, the argon partial pressure  
301 at this level does not seem to have an important effect on the measured krypton isotopic ratios,  
302 which may be counter-intuitive.

303  
304 However, the krypton trapping temperature seems to have a non-negligible effect. For example,  
305 the normalized  $^{86}\text{Kr}/^{84}\text{Kr}$  ratio is significantly higher for a krypton trapping temperature of 75  
306 K ( $1.0094 \pm 0.0017$  with one trap and  $1.0041 \pm 0.0016$  with two traps) than for experiments at  
307 68 K or 70 K (Figure 7). In particular, the isotopic fractionation when using only one trap is  
308 significantly larger compared to using the dual trap. Although uncertainties are larger, similar  
309 observations can be drawn for the other krypton isotopic ratios (Figure 7).

310  
311 The increase in  $^{86}\text{Kr}/^{84}\text{Kr}$  is compatible with expectations that as the krypton trapping  
312 temperature is increased, more krypton is lost in the argon fraction, with the lost fraction  
313 preferentially enriched in the lighter isotopes (lower measured  $^{84}\text{Kr}$  abundances, figure 7). As  
314 can be seen in figure 2, using a distillation temperature of 75 K for separating Ar from Kr, a  
315 small fraction of krypton is lost with argon (Figure 7).

316  
317 Hence, rather than minimizing the argon fraction in krypton, maximizing the recovered krypton  
318 fraction will provide more accurate Kr isotopic data, even if this marginally increases the argon  
319 fraction in krypton. Using a distillation temperature below 70 K (between 67 K and 70 K) for  
320 separating argon from krypton should provide the best Kr abundance and isotopic data.  
321 Therefore, given that variations in Ar partial pressure by over a factor of ten has very limited  
322 effect on measured krypton isotopic ratios, we recommend analyzing  $\geq 98\%$  of the Kr aliquot  
323 for the most accurate Kr isotopic ratio measurements, especially when using a single stainless  
324 steel trap where the krypton isotopic fractionation appears to be larger.

## 325 326 327 **Conclusion**

328  
329 The protocol described in this study using the new cryogenic system, combined with  
330 temperature cycling of the trap, allows a clean separation of the heavy noble gases (Ar, Kr, Xe)  
331 with less than 1 % of one gas phase in another gas phase. We recommend maximizing the  
332 recovered krypton fraction even if this increases the argon fraction in krypton so as not to  
333 fractionate krypton isotopes during Ar-Kr separation. The reproducibility of air standards with  
334 this protocol is high with precisions on measured isotopic ratios reaching 3-7 ‰ for low  
335 abundant isotopes (such as  $^{78}\text{Kr}/^{84}\text{Kr}$  and  $^{128}\text{Xe}/^{130}\text{Xe}$ ). The protocol should allow for more  
336 accurate determinations of the krypton and xenon isotopic compositions of samples with very  
337 low krypton and xenon abundances such as oceanic basalts.

## 338 339 **Conflicts of interest**

340  
341 The authors declare no conflict of interest.

## 342 343 **Acknowledgements**

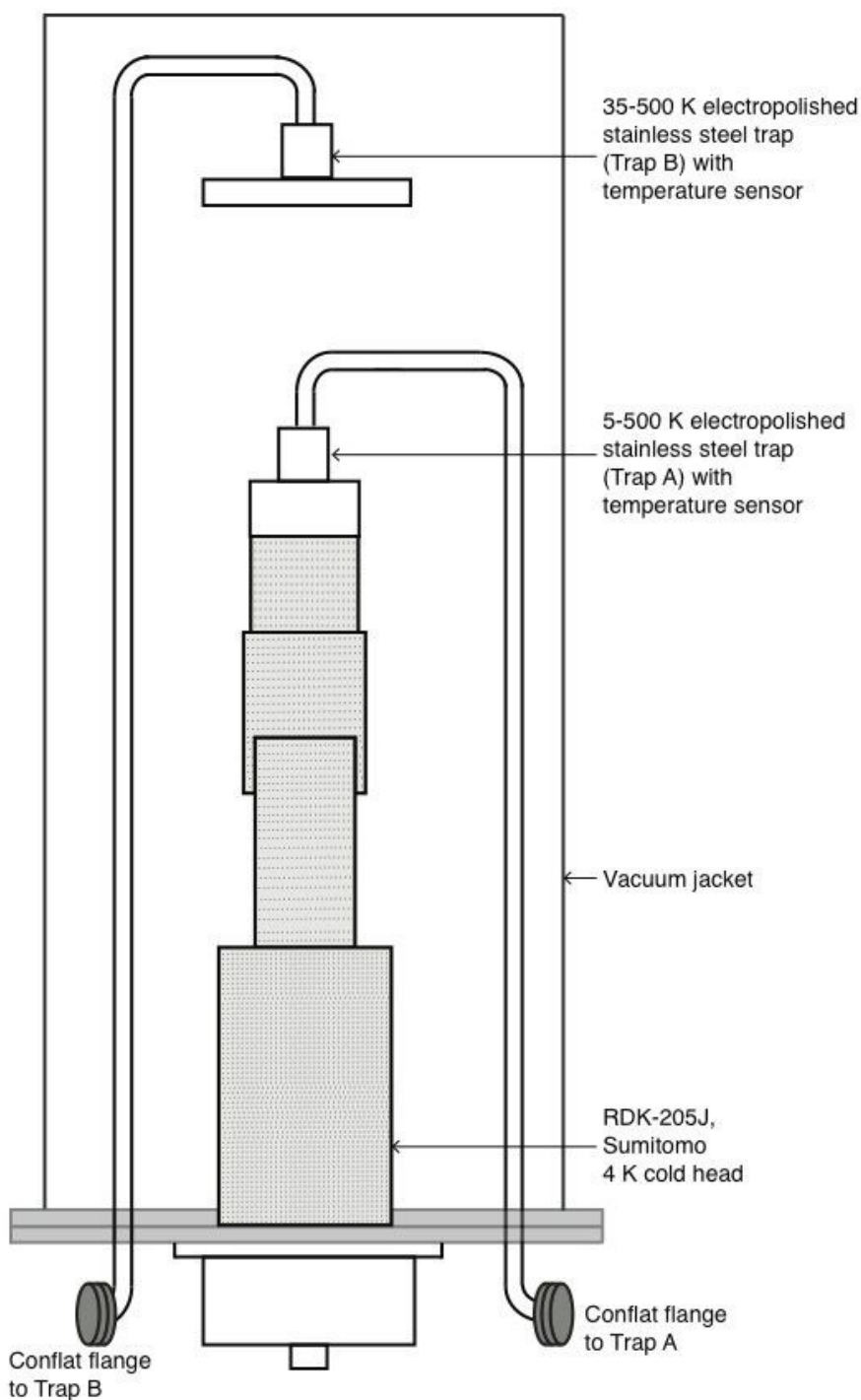
344  
345 The authors are grateful to Magdalena Huyskens for constructive comments and discussion on  
346 the first versions of this manuscript.

**References**

1. Ozima M, Podosek FA. Noble Gas Geochemistry. Cambridge University Press; 2002.
2. Burnard P. The Noble Gases as Geochemical Tracers. In: Hoefs J, editor. *Advances in Isotope Geochemistry*. Springer-Verlag Berlin Heidelberg; 2013.
3. Porcelli D, Ballentine CJ, Wieler R. Noble Gas Geochemistry and Cosmochemistry. *Rev Mineral Geochemistry* [Internet]. 2002 Jan 1;47(1):1–19. Available from: <https://doi.org/10.2138/rmg.2002.47.1>
4. Mukhopadhyay S, Parai R. Noble Gases: A Record of Earth's Evolution and Mantle Dynamics. *Annu Rev Earth Planet Sci* [Internet]. 2019 Jun 3;47(1):389–419. Available from: <https://doi.org/10.1146/annurev-earth-053018-060238>
5. Moreira M. Noble Gas Constraints on the Origin and Evolution of Earth's Volatiles. *Geochemical Perspect* [Internet]. 2013;2(2):229–403. Available from: <http://perspectives.geoscienceworld.org/content/2/2/229.abstract>
6. Marty B. The origins and concentrations of water, carbon, nitrogen and noble gases on Earth. *Earth Planet Sci Lett* [Internet]. 2012;313--314:56–66. Available from: <http://www.sciencedirect.com/science/article/pii/S0012821X11006388>
7. Crowther SA, Mohapatra RK, Turner G, Blagburn DJ, Kehm K, Gilmour JD. Characteristics and applications of RELAX, an ultrasensitive resonance ionization mass spectrometer for xenon. *J Anal At Spectrom* [Internet]. 2008;23(7):938–47. Available from: <http://dx.doi.org/10.1039/B802899K>
8. Crowther SA, Gilmour JD. Measuring the elemental abundance and isotopic signature of solar wind xenon collected by the Genesis mission. *J Anal At Spectrom* [Internet]. 2012;27(2):256–69. Available from: <http://dx.doi.org/10.1039/C1JA10163C>
9. Burnard P, Zimmermann L, Sano Y. The Noble Gases as Geochemical Tracers: History and Background. In: Burnard P, editor. *The Noble Gases as Geochemical Tracers* [Internet]. Berlin, Heidelberg: Springer Berlin Heidelberg; 2013. p. 1–15. Available from: [https://doi.org/10.1007/978-3-642-28836-4\\_1](https://doi.org/10.1007/978-3-642-28836-4_1)
10. Reynolds JH, Jeffery PM, McCrory GA, Varga PM. Improved charcoal trap for rare gas mass spectrometry. *Rev Sci Instrum*. 1978;49:547–8.
11. Lott DE, Jenkins WJ. An automated cryogenic charcoal trap system for helium isotope mass spectrometry. *Rev Sci Inst* . 1984;55:1982-1988.
12. Lott DEIII. Improvements in noble gas separation methodology: a nude cryogenic trap. G-cube. 2001;2001GC0002.
13. Moreira M, Rouchon V, Muller E, Noirez S. The xenon isotopic signature of the mantle beneath Massif Central. *Geochemical Perspect Lett* [Internet]. 2018;6:28–32. Available from: <http://www.geochemicalperspectivesletters.org/article1805>
14. Busemann H, Baur H, Wieler R. Primordial noble gases in “phase Q” in carbonaceous and ordinary chondrites studied by closed-system stepped etching. *Meteorit Planet Sci* [Internet]. 2000;35(5):949–73. Available from: <http://dx.doi.org/10.1111/j.1945-5100.2000.tb01485.x>
15. Riebe MEI, Busemann H, Wieler R, Maden C. Closed System Step Etching of CI chondrite Ivuna reveals primordial noble gases in the HF-solubles. *Geochim Cosmochim Acta* [Internet]. 2017;205:65–83. Available from: <http://www.sciencedirect.com/science/article/pii/S0016703717300819>
16. Broadley MW, Barry PH, Bekaert D V, Byrne DJ, Caracausi A, Ballentine CJ, et al. Identification of chondritic krypton and xenon in Yellowstone gases and the timing of terrestrial volatile accretion. *Proc Natl Acad Sci* [Internet]. 2020 Jun 4;202003907. Available from: <http://www.pnas.org/content/early/2020/06/03/2003907117.abstract>
17. Bekaert D V, Marrocchi Y, Meshik A, Remusat L, Marty B. Primordial heavy noble

- 1  
2  
3 400 gases in the pristine Paris carbonaceous chondrite. *Meteorit Planet Sci* [Internet]. 2019 Feb 1;54(2):395–414. Available from: <https://doi.org/10.1111/maps.13213> Article Online  
DOI: 10.1039/D0JA00052C
- 4 401
- 5 402 18. Stanley RHR, Baschek B, Lott III DE, Jenkins WJ. A new automated method for  
6 403 measuring noble gases and their isotopic ratios in water samples. *Geochemistry,  
7 404 Geophys Geosystems* [Internet]. 2009 May 1;10(5). Available from:  
8 405 <https://doi.org/10.1029/2009GC002429>
- 9 406 19. Sumino H. History and Current Status of Noble Gas Mass Spectrometry to Develop  
10 407 New Ideas Based on Study of the Past. *J Mass Spectrom Soc Jpn.* 2015;63(1):1–30.
- 11 408 20. Moreira M, Kunz J, Allègre CJ. Rare gas systematics on popping rock : estimates of  
12 409 isotopic and elemental compositions in the upper mantle. *Science.* 1998;279:1178–81.
- 13 410 21. Mukhopadhyay S. Early differentiation and volatile accretion recorded in deep-mantle  
14 411 neon and xenon. *Nature* [Internet]. 2012;486:101–4. Available from:  
15 412 <http://dx.doi.org/10.1038/nature11141>  
16 413  
17 414  
18 415

416 **Figure 1.** Schematic of the dual stainless steel cryogenic trap fabricated by Janis Research  
417 Company. The design is considered proprietary by Janis Research, therefore the full schematic  
418 is not shown.



437 **Figure 2.** Release curves of Ne, Ar, Kr, Xe from the stainless steel traps. The release curves of  
438 Ar, Kr and Xe were determined with different protocols (see the experimental procedure and  
439 figure 3). The dashed grey lines highlight the overlap of the release curves at 70 K and 90 K.  
440

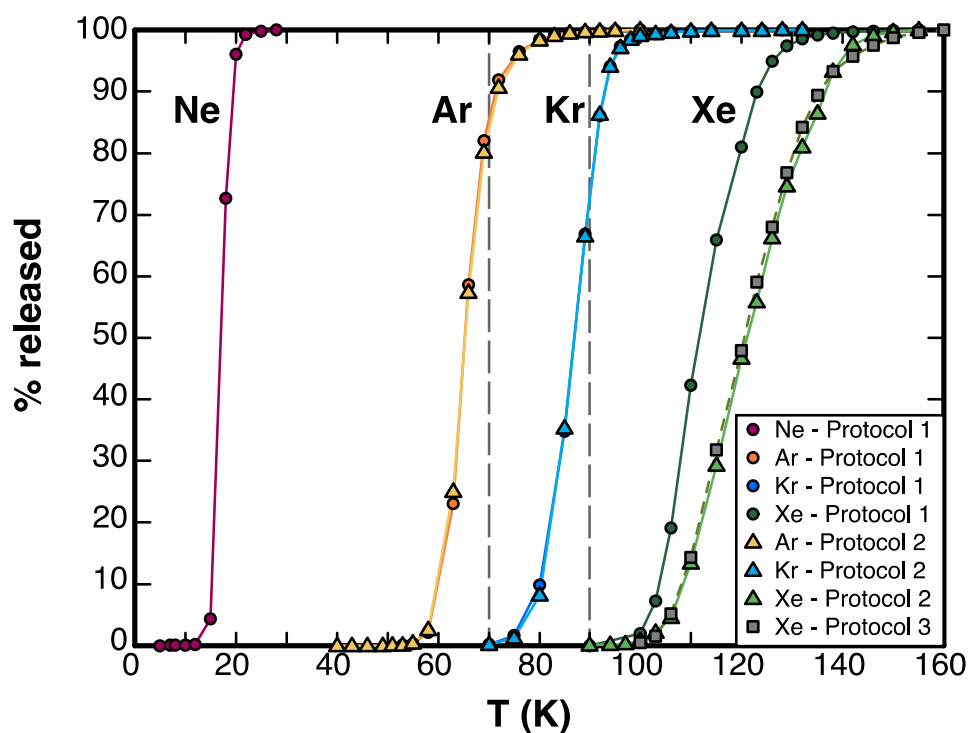


**Figure 3.** Flow chart describing the sequence of the three protocols. As mentioned in the text, a temperature cycle takes about 30 minutes, the total duration of the protocols (purification and separation) without taking into account the mass spectrometry analysis time is indicated at the top. We note that no time is needed in advance to allow the traps to reach 25 K and 70 K respectively as the system can be cooled down from 200 K to 25 K for Trap A and to 70 K for Trap B in less than 30 minutes (i.e., during the purification).

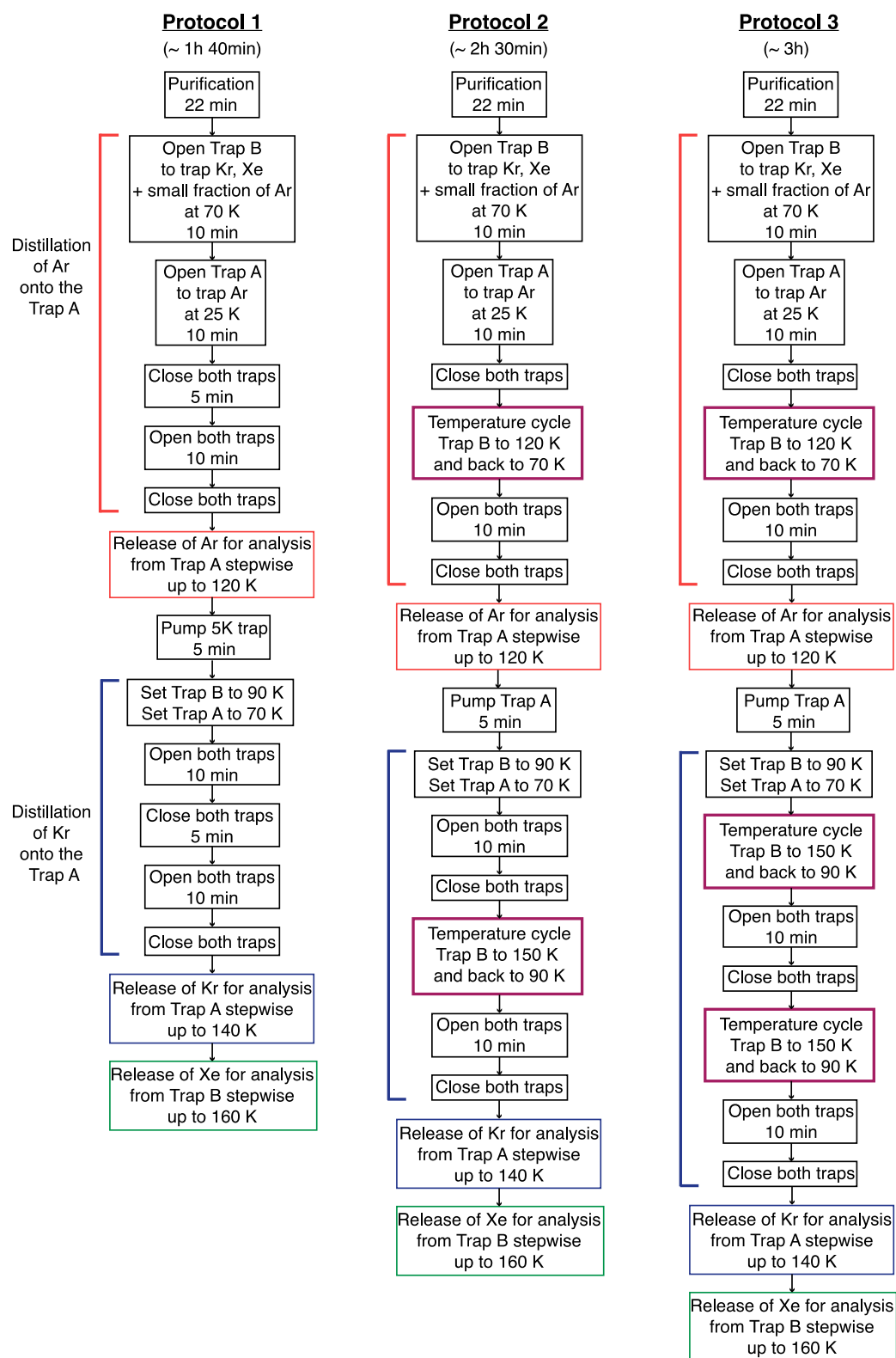
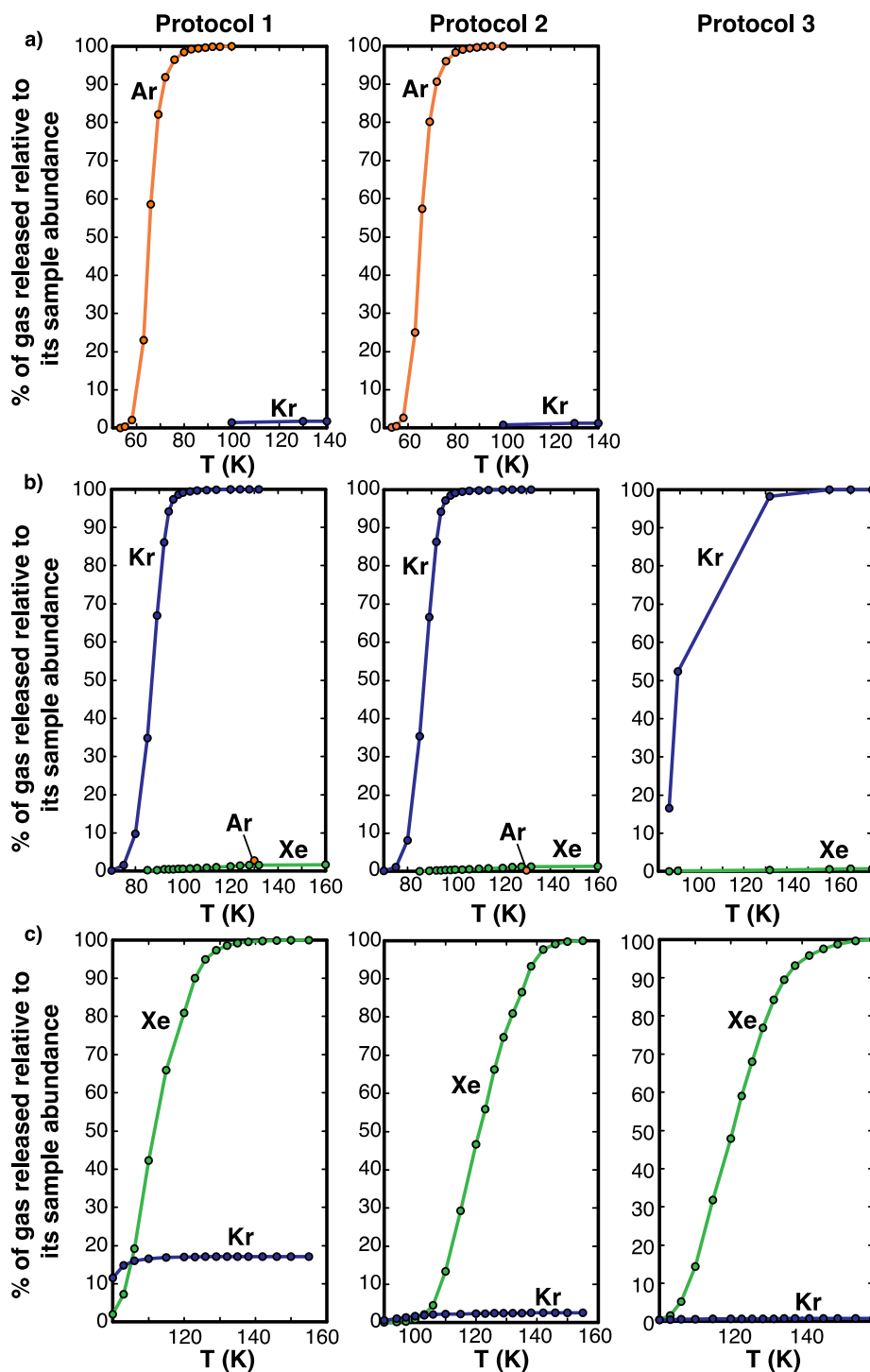
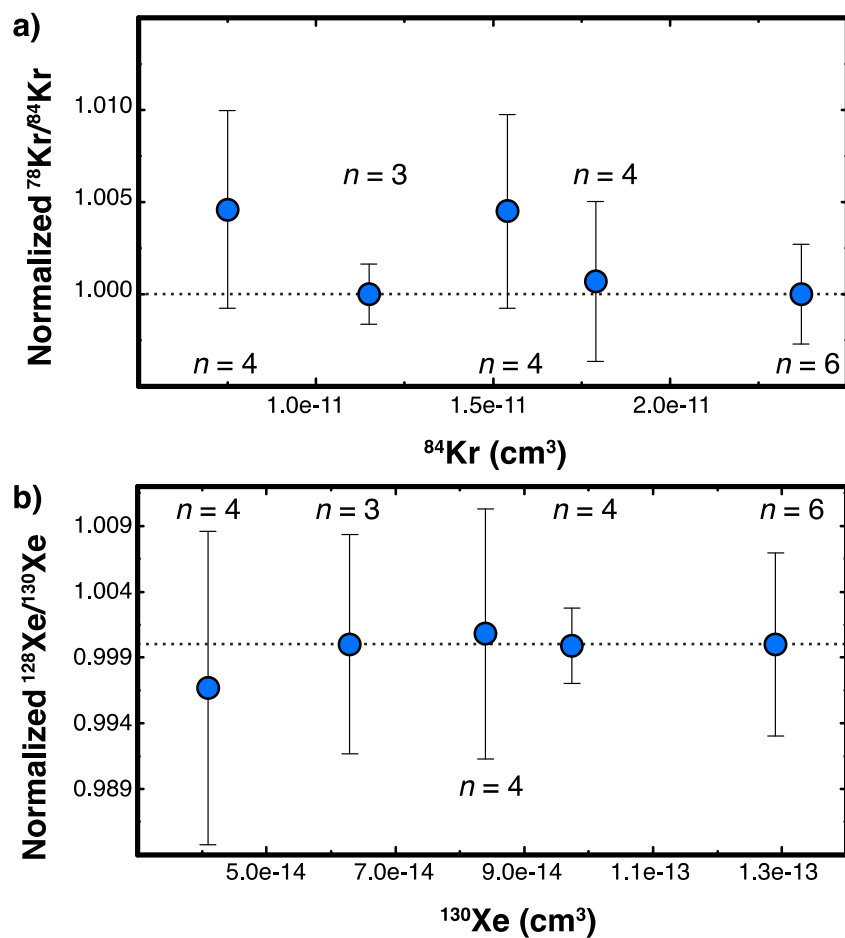


**Figure 4.** Step-release of the gases with the different protocols (Protocols 1, 2 and 3 in Figure 3). The figures show in row a) the Ar release from Trap A and the proportion of Kr in Ar, in row b) the Kr release from Trap A with the proportions of Ar and Xe in Kr, in row c) the Xe release from Trap B with the proportions of Kr in Xe. The percentage of one gas corresponds to the fraction of its total abundance in the sample (refer to Table 1, rows 2, 3 and 4 for the precise values). The x-axes have different scales on the sub-figures. Note the contrast in the degree of separation of the heavy noble gases compared to figure 2 and between Protocol 1 and Protocol 2.



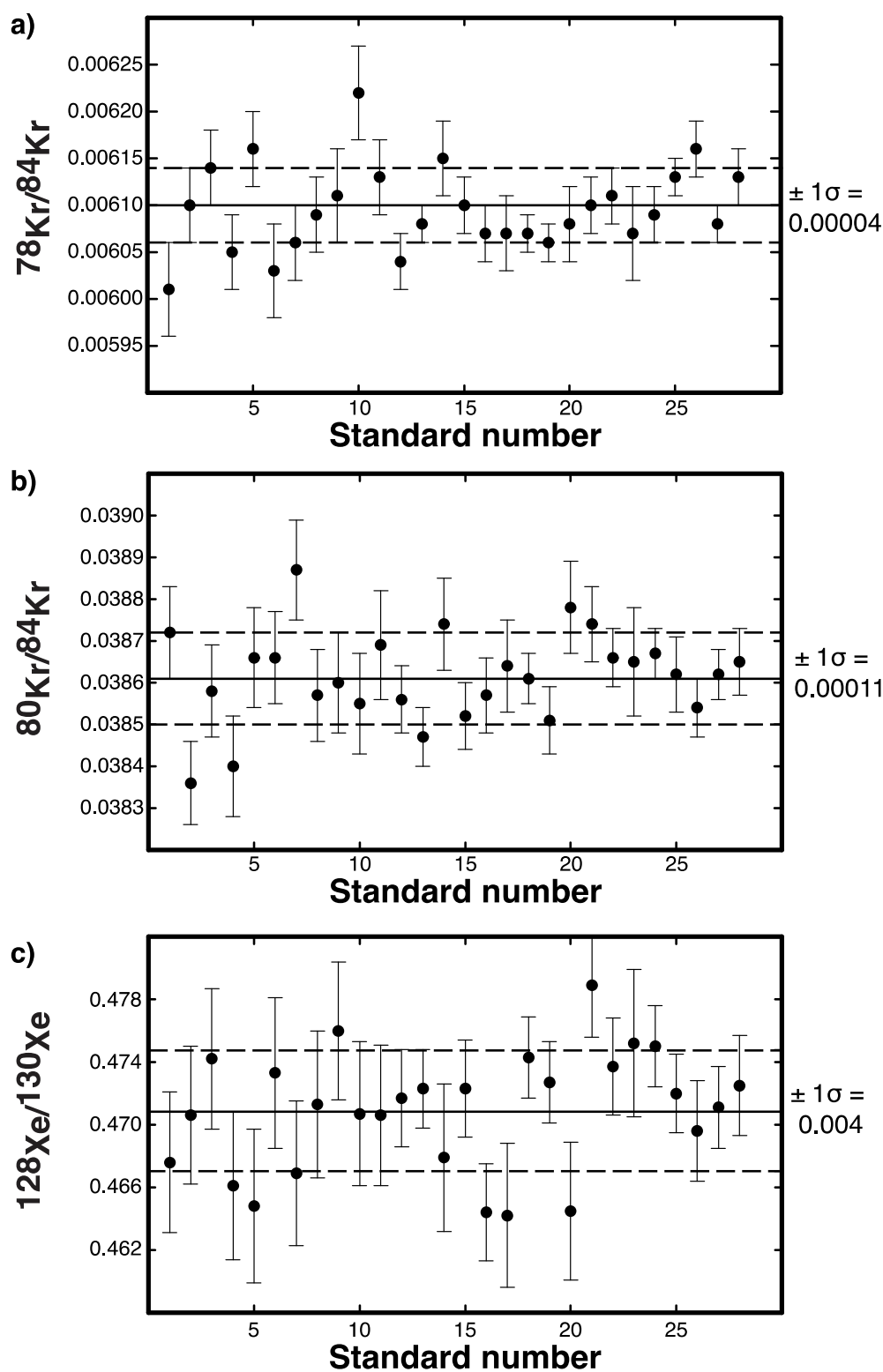


587 **Figure 5.** External reproducibility of (a)  $^{78}\text{Kr}/^{84}\text{Kr}$  and (b)  $^{128}\text{Xe}/^{130}\text{Xe}$  ratios obtained for  
 588 different aliquots of the air standard with the distillation and one temperature cycling protocol.  
 589 To observe the deviation from linearity, the ratios are normalized to the average of the largest  
 590 standard. Each dot is the average of  $n$  analyses and the error shown is the standard deviation.  
 591



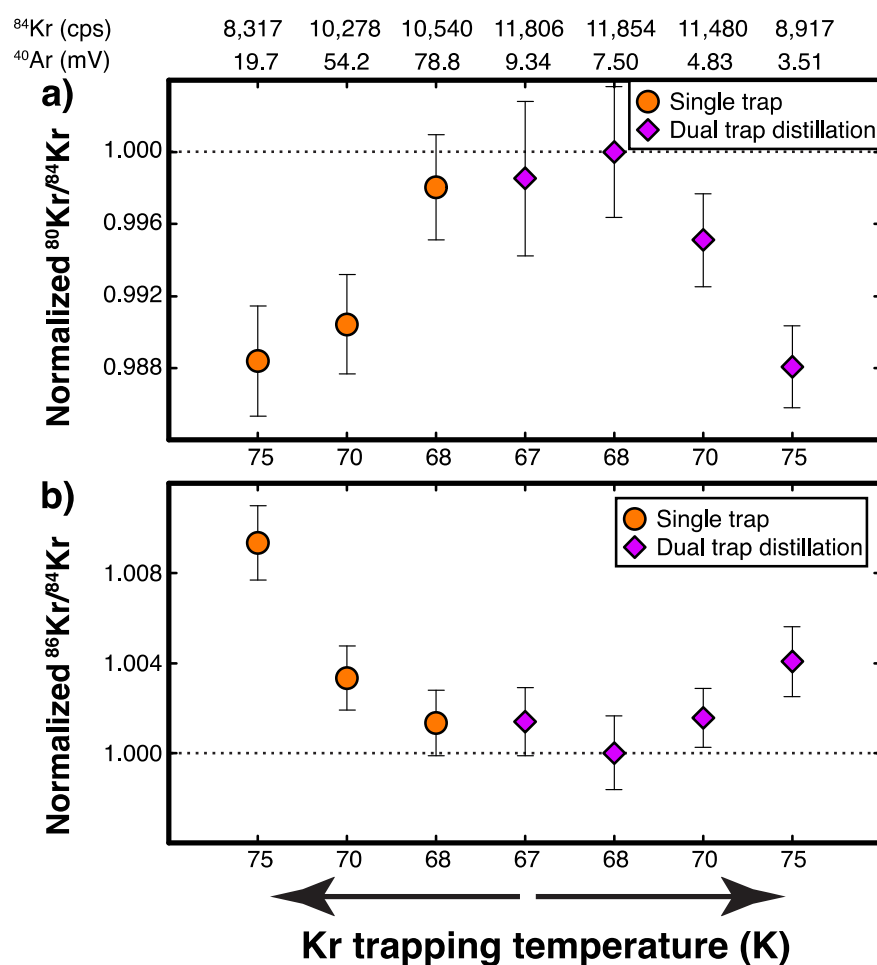
592  
593  
594  
595  
596  
597  
598  
599  
600  
601  
602  
603  
604  
605  
606  
607  
608  
609

610 **Figure 6.** Reproducibility of Kr and Xe isotopic ratios from air standard aliquots of different  
611 sizes. a)  $^{78}\text{Kr}/^{84}\text{Kr}$ , b)  $^{80}\text{Kr}/^{84}\text{Kr}$  and c)  $^{128}\text{Xe}/^{130}\text{Xe}$ . This set of standards was measured over  
612 13 days with Protocol 2 and include three standard sizes, ranging from  $7.52 \times 10^{-12}$  cc to  $2.37 \times 10^{-11}$   
613 cc of  $^{84}\text{Kr}$  and from  $4.1 \times 10^{-14}$  cc to  $1.29 \times 10^{-13}$  cc of  $^{130}\text{Xe}$ .  
614



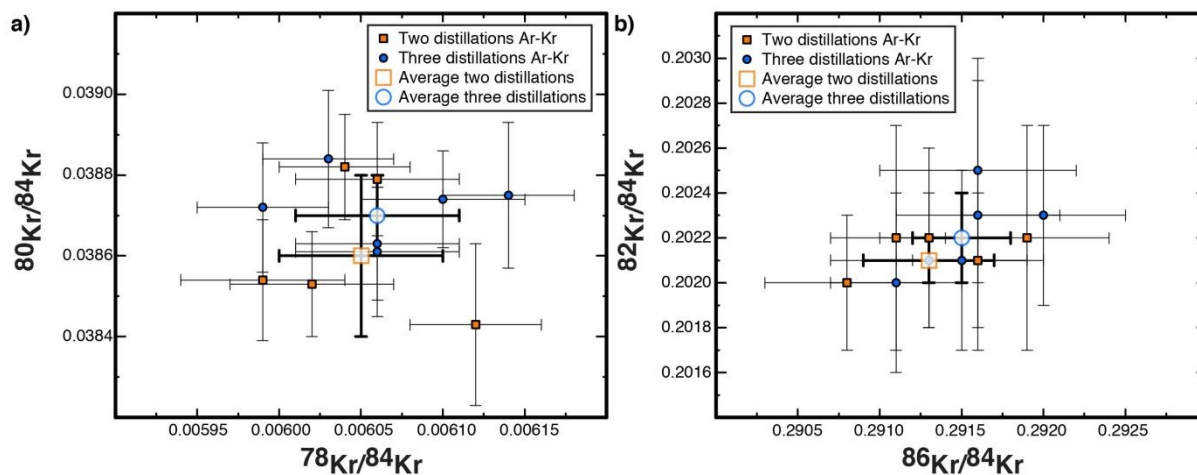
615  
616  
617  
618

619 **Figure 7.** Krypton isotopic ratios depending on the krypton trapping temperature and the argon  
 620 partial pressure (as determined by the abundance of  $^{40}\text{Ar}$  in the mass spectrometer) for air  
 621 standard aliquots of the same size (aliquots with  $1.1 \times 10^{-7} \text{ cm}^3$  of  $^{40}\text{Ar}$  and  $7.5 \times 10^{-12} \text{ cm}^3$  of  
 622  $^{84}\text{Kr}$ ). a)  $^{80}\text{Kr}/^{84}\text{Kr}$  and b)  $^{86}\text{Kr}/^{84}\text{Kr}$ , each ratio is the average of 4 to 9 analyses, the error bars  
 623 being the standard deviations on these 4 to 9 analyses. In order to show the fractionation, the  
 624 ratios are normalized to the one measured at 68 K using the distillation technique. The measured  
 625  $^{84}\text{Kr}$  signal (in cps) is indicated at the top as well as the amount of  $^{40}\text{Ar}$  (in mV) measured after  
 626 Kr. Experiments using only the Trap A are represented with orange circles and experiments  
 627 using the two traps with the distillation technique are in purple diamonds. Note that for better  
 628 comparison of the results, the temperature on the x-axis increase on both sides from a middle  
 629 point at 67 K.  
 630



631  
 632  
 633  
 634  
 635  
 636  
 637

638 **Figure 8.** Krypton isotopic ratios for separation experiments involving two Ar-Kr distillations  
 639 with one temperature cycle (orange square) and three Ar-Kr distillations with two temperature  
 640 cycles (blue circle) for air standard aliquots of the same size (aliquots with  $1.1 \times 10^{-7} \text{ cm}^3$  of  $^{40}\text{Ar}$   
 641 and  $7.5 \times 10^{-12} \text{ cm}^3$  of  $^{84}\text{Kr}$ ). a)  $^{80}\text{Kr}/^{84}\text{Kr}$  and  $^{78}\text{Kr}/^{84}\text{Kr}$  and b)  $^{82}\text{Kr}/^{84}\text{Kr}$  vs  $^{86}\text{Kr}/^{84}\text{Kr}$ . The only  
 642 difference between the two sets of experiments is the number of Ar-Kr distillation and  
 643 temperature cycle. The two distillation experiment has been repeated five times, and the three  
 644 distillation experiment six times. The average for each set of experiment is shown with the  
 645 bigger open symbol and bold uncertainties. The partial pressure of Ar in the mass spectrometer  
 646 was 1.8 times lower for the three distillation experiments than for the two distillation  
 647 experiments. The Kr isotopic ratios are similar for all the analyses.



648  
 649  
 650  
 651  
 652  
 653  
 654  
 655  
 656  
 657  
 658  
 659  
 660  
 661

**Table 1.** Level of separation of heavy noble gases (Ar, Kr, Xe) with the new cryogenic system. The percentages refer to the percent abundance of one gas relative to its total abundance in the sample. Different protocols have been applied with a varying number of temperature cycling steps and slightly different distillation temperatures (see the experimental procedure) to compare the efficiency of heavy noble gas separation. The temperature  $T_1$  refers to the distillation temperature of Ar from Kr and  $T_2$  to the distillation of Kr from Xe. The results show that one temperature cycling drastically improves Ar, Kr, Xe separation. *n.a.* not analyzed. Uncertainties, estimated from the uncertainties on the measured abundances, are less than 0.2 %.

Protocols	Protocol number in Figure 3	Kr in Ar	Ar in Kr	Xe in Kr	Kr in Xe
Single trap, no cycling (estimated based on the release curves, $T_1 = 70$ K, $T_2 = 90$ K)		< 2 %	14.6 %	< 2 %	26.7 %
Dual trap, no cycling, step-release ( $T_1 = 70$ K, $T_2 = 90$ K)	Protocol 1	1.8 %	2.7 %	1.7 %	17.2 %
Dual trap, 1 cycling, step-release ( $T_1 = 70$ K, $T_2 = 90$ K)	Protocol 2	1.2 %	0.2 %	1.4 %	2.6 %
Dual trap, 2 cycling (Kr-Xe), step-release ( $T_1 = 70$ K, $T_2 = 90$ K)	Protocol 3	1.5 %	<i>n.a.</i>	0.7 %	0.8 %
Dual trap, 1 cycling, single release ( $T_1 = 70$ K, $T_2 = 95$ K)	Protocol 2	3.7 %	0.2%	3.6 %	0.4 %
Dual trap, 1 cycling, single release ( $T_1 = 67$ K, $T_2 = 92$ K)	Protocol 2	0.7 %	0.5 %	1.2 %	0.9 %